Int. J. Electrochem. Sci., 15 **(2020)** 10382 – 10391, doi: 10.20964/2020.10.27

International Journal of
ELECTROCHEMICAL
SCIENCE
www.electrochemsci.org

Short Communication

Investigation of Pt/C and Pt-Ru/C Mixed Catalyst for DME Oxidation in Direct Dimethyl Ether Fuel Cells

Lehong Xing[*], *Yixin Wang, Xinting Shi, Rui Dong, Lin Wu*

College of Chemistry and Chemical Engineering, Mu Danjiang Normal University,
[*]E-mail: xinglehonghit@163.com

Received: 2 June 2020 / *Accepted:* 24 July 2020 / *Published:* 31 August 2020

The performance of Pt/C and Pt-Ru/C mixed catalyst has been studied for dimethyl ether (DME) oxidation in direct dimethyl ether fuel cells (DDFCs). Transmission Electron Microscopy (TEM) characterizations show that Pt and Pt-Ru particles (about 3.0 nm) are highly dispersed on their supports. The electrochemical activity of mixed catalyst was evaluated by polarization curve, amperometric current density – time technique, and electrochemical impedance spectroscopy (EIS). The results show that the activity of mixed catalyst is better than Pt/C toward DME oxidation. Pt-Ru/C in the mixed catalyst is helpful for reducing the catalyst poisoning effect, and simultaneously, Pt/C in the mixed catalyst can provide continuous Pt active sites for DME dehydrogenation. Too much Pt-Ru can reduce the catalytic activity. The optimal Pt-Ru content is 3.5 mg cm^{-2} Pt and 0.5 mg cm^{-2} Pt-Ru (metal loading) in anode catalyst layer.

Keywords: Direct dimethyl ether fuel cell; Dimethyl ether; Anode catalyst; Pt-Ru/C; Pt/C

1. INTRODUCTION

Direct type fuel cells which use formic acid, ethanol, formaldehyde, methanol and dimethyl ether (DME) as their fuel have been widely studied recently as potential new power sources [1-3]. These investigated direct type fuel cells are all have their own advantages [4,5]. The direct dimethyl ether fuel cell (DDFC) is one of the promising fuel cells [6]. Dimethyl ether (DME) is the simplest ether and there is no C-C bond in its molecular (CH_3OCH_3) [7]. The toxity of DME is low. DME gas can be compressed easily into liquid form, so that the transportation of DME is convenient. The energy density of DME is high and its fuel crossover effect is low [8,9]. However, DDFC still has some obstacles which hinder its practical applications. The major obstacle limits the performance of DDFC is the poor kinetics of DME oxidation, which mainly results from the week adsorption of DME on catalyst and the poisoning effect of Pt based catalyst [10]. The development of active catalyst towards DME oxidation is very necessary for DDFC. Pt-Ru/C and Pt/C are the two most commonly used anode catalyst for DDFC. Different researchers have different conclusions about which one is more proper for DME oxidation. Liu [11] compare the performance of the two catalyst in DDFC. They find that Pt-Ru/C is better than Pt/C in low over potential range. Oppositely, Pt/C is better than Pt-Ru/C in high over potential range. In low over potential range, the anode needs OH supported by Ru to remove absorbed CO. In high over potential range, the absorbed CO can be oxidized immediately and the Ru addition decreases the continuous Pt active sites, which is harmful for DME oxidation. Kerangueven [12] find that Ru content in Pt-Ru has an important influence on the performance of DDFC. DDFC performs better with the decrease of Ru content in Pt-Ru. Tsutsumi [13] compare the two catalyst at different temperatures. The activity of Pt-Ru is better than Pt at high temperature, because the rate of DME oxidation reaction is relatively fast at high temperate and there are lots of adsorbed posing species generated on the surface of catalyst. Ru is helpful for the removal of posing intermediates. At low temperature, the activity of Pt is better than Pt-Ru, because the catalyst posing effect is not very significant. Li [14] consider that the catalyst activity of Pt-Ru is higher than Pt, and the optimal Pt to Ru ration is $Pt_{0.8}Ru_{0.2}$. Based on the above results, there are two different (positive and negative) effects of Ru on the activity of DME oxidation. The positive one is that Ru is helpful for the generation of oxygen-containing species. These oxygen-containing species can promote the catalyst activity when the oxidation of posing intermediates is the rate-determing step for DME oxidation reaction. The negative one is that the presence of Ru decreases the continuous Pt active sites, which is bad for DME adsorption and following dehydrogenation. It is very necessary to develop a catalyst which can make ideal balance between positive and negative effects. Besides, which one of these two effects (positive and negative) plays a major role in DME oxidation is strongly impacted by the operating conditions. Up to now, most of the researches about Pt-Ru/C and Pt/C catalyst are carrying out under high temperature and pressure. The performances of DDFCs with the two catalysts at lower than 100 °C under ambient pressure have not been studied in detail. In this work, Pt-Ru/C is added into Pt/C to form a mixed catalyst for DME oxidation. We represent the first systematic study of the mixed catalyst with different Pt-Ru/C content at 60 °C under ambient pressure. The mixed catalyst can provide continuous Pt active sites for DME dehydrogenation, and simultaneously provide oxygen-containing species for adsorbed intermediates oxidation. The influence of mixed catalyst on the performance of DDFC has been discussed based on the results of multiple physical and electrochemical tests.

2. EXPERIMENTAL

2.1. Preparation of catalyst

The 40 mass% Pt/C were synthesized by microwave-assisted polyol process [15]. 60 mg of pretreated carbon black (Vulcan XC-72) was ultrasonically dispersed in the solution containing 12 ml isopropyl alcohol and 48 ml glycol (EG) to form a uniform ink. 5.4 ml of 0.0386 mol L^{-1} H_2PtCl_6-EG solution dissolved in the above ink under stirring for 2h. 1 mol L^{-1} NaOH-EG solution was used to adjust the pH. The pH value of the solution was about 12. Afterwards, the solution was heated by a microwave oven (2450MHz, 800W) for 55s under argon gas protection. The solution was cooled down to ambient temperature under stirring. Then 0.1 mol L^{-1} HNO_3 solution was used to adjust the pH. The pH value of the solution was about 3. The resulting catalyst was washed with ultrapure water, and then dried for 4 h at 80 °C in vacuum. The 40 mass% Pt-Ru/C was synthesized in a similar way mentioned above with H_2PtCl_6-EG solution and $RuCl_3$-EG solution as precursors.

2.2. Preparation of Membrane electrode assembly (MEA)

The MEAs (5 cm^2) were prepared using a typical process which had been reported in detail previously[16]. The anode gas diffusion layers (GDLs) were wet-proofed carbon papers (Toray, TGP-H-060). The PTFE content in anode GDLs was 18 mass%. The wet-proofed cathode GDLs were composed of carbon papers and 1 mg cm^{-2} of Vulcan XC-72 carbon black. The PTFE content in cathode GDLs was 30 mass%. Pt/C and Pt-Ru/C mixed catalysts were used as the anode catalysts. The Pt and Pt-Ru loading of different MEAs are listed in Table 1. The total metal loading in anode catalyst layers of these MEAs are 4 mg cm^{-2}. The cathode catalyst was Pt/C (2 mg cm^{-2}). Nafion content in catalyst layers were 20 mass%.

Table 1. Components of anode catalyst layers for different MEAs.

Samples	Pt/ mg cm^{-2}	Pt-Ru/ mg cm^{-2}
MEA-1	4.0	0
MEA-2	3.5	0.5
MEA-3	3.8	0.2
MEA-4	3.0	1.0

2.3. Electrochemical measurements

2.3.1 Steady-state polarization curves

A Potentiostat/Galvanostat apparatus (Hokuto Denko Inc. HA-151) was employed to record the steady-state polarization curves of DME oxidation [17]. At the anode side, 1.5 mol L^{-1} DME solution was fed with a flow rate of 3 mL min^{-1}. Simultaneously, the humidified H_2 was supplied to cathode with a flow rate of 200 mL min^{-1}. The cathode served as a dynamic hydrogen electrode (DHE).

2.3.2 Electrochemical impedance spectra (EIS)

The EIS of the anodes was measured by an electrochemical analysis instrument (Shanghai Chen-Hua Instruments Corp., CHI 604B) under 0.45 V vs. DHE at 60 °C. The amplitude of sinusoidal potential signal was 5mV. The frequencies were from 1 kHz to 0.01 Hz.

2.3.3 Amperometric i–t curves

The amperometric *i–t* curves of DME oxidation were measured by CHI 604B at 0.45 V vs. DHE. The anode and cathode reactants used in above electrochemical measurements (steady-state polarization curves, EIS, amperometric *i–t*) were all the same.

2.3.4 Fuel cell testing

The performances of DDFCs with different anode catalyst were tested using a commercial electrochemical station (Arbin Fuel Cell Testing System) at 60°C under ambient pressure. During the test, 1.5 mol L^{-1} DME solution was fed at a flow rate of 3 mL min^{-1}, while humidified oxygen was supplied at a flow rate of 200 mL min^{-1}.

3. RESULTS AND DISCUSSION

TEM images and the nanoparticle size distribution diagrams of catalysts are presented in Fig. 1 and Fig. 2. The size distribution diagrams are obtained by random measurements of 100 particles. Pt and Pt-Ru alloy particles are highly dispersed on supports. The average particles sizes of the two catalysts are nearly the same (about 3 nm). Fig. 3 shows the polarization curves and the power density curves of MEAs with or without Ru in anode catalyst at 60 °C. The maximum power density of the MEA1 and MEA2 is 40 mW cm^{-2} and 50 mW cm^{-2}, respectively. The performance of MEA with mixed catalyst is higher than that of Pt/C. The Ru in mixed catalyst provides oxygen-containing species which is helpful for the oxidation of absorbed intermediates and decrease the catalyst posing effect. The Pt/C in mixed catalyst provides continuous Pt active sites for DME oxidation. The mixed catalyst can make a balance between the positive and negative effects.

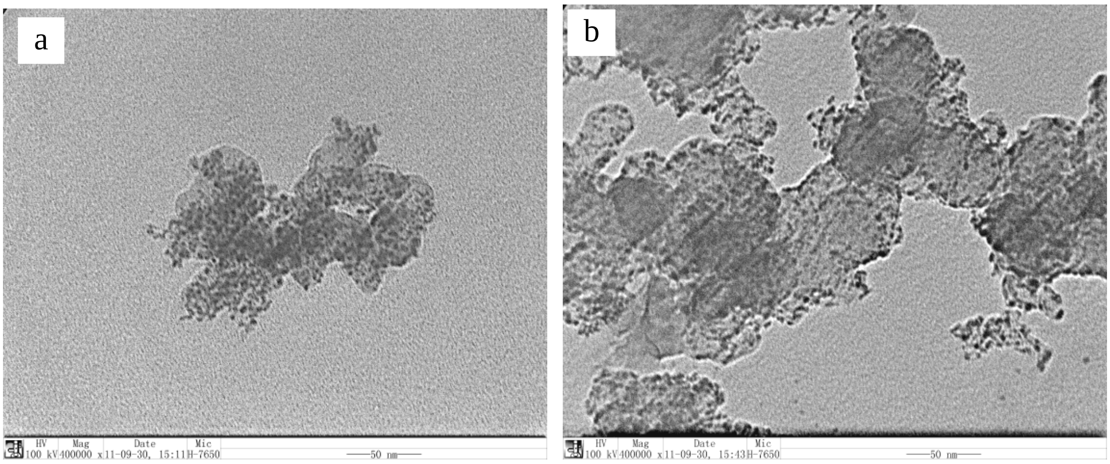

Figure 1. TEM images of catalysts: (a) Pt/C; (b) Pt-Ru/C.

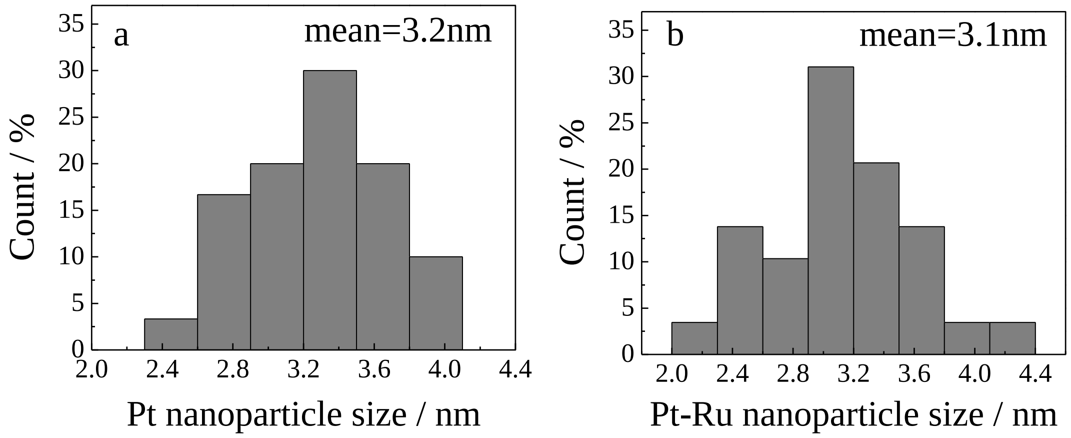

Figure 2. Size distribution diagrams of catalysts: (a) Pt/C ; (b) Pt-Ru/C.

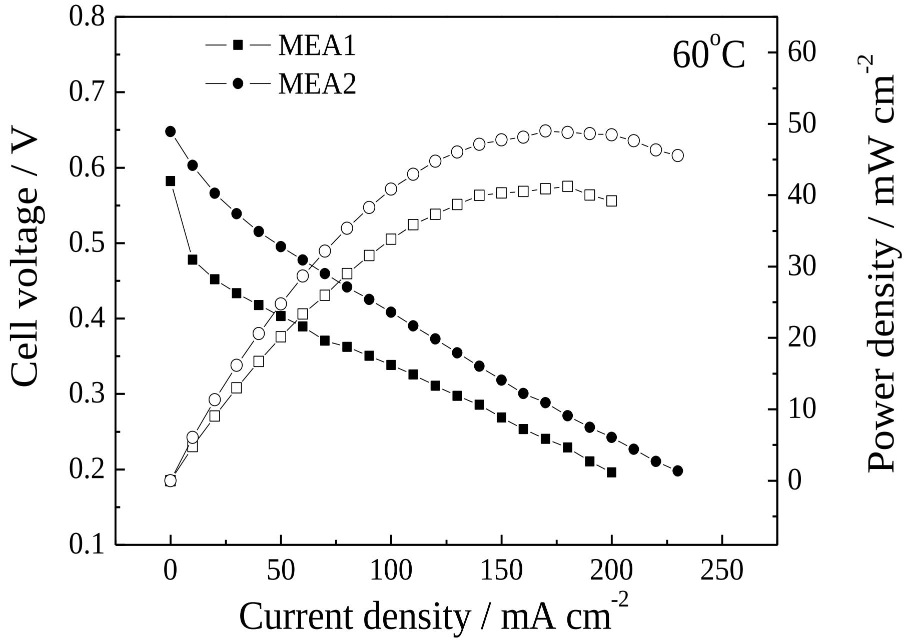

Figure 3. The polarization curves and the power density curves of the MEAs with different anode catalysts at 60 °C: MEA1 with Pt/C；MEA2 with the mixed catalysts.

Fig. 4 shows the polarization curves of DME oxidation at different anode. The performance of MEA2 is better than that of MEA1. MEA2 with the mixed catalysts exhibits lower polarization at anode. The Ru in mixed catalyst is benefit to decrease polarization and improve the performance of DDFC.

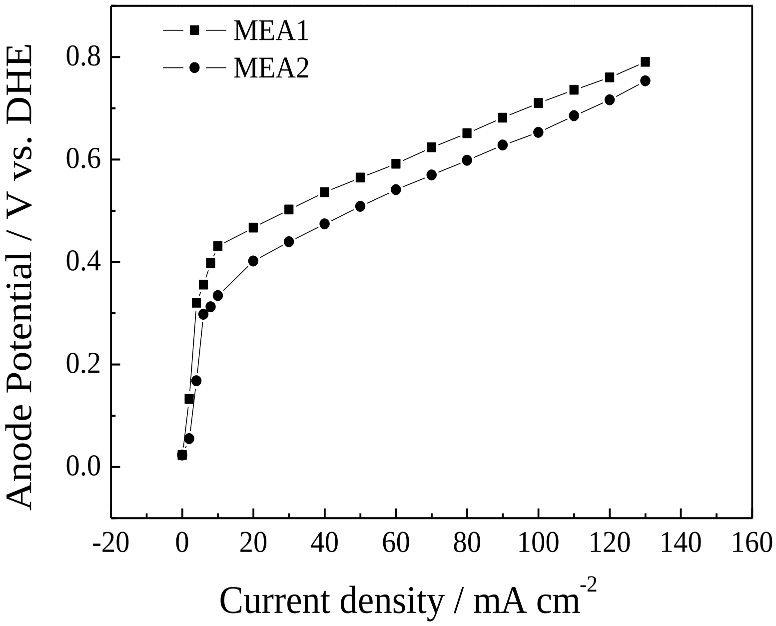

Figure 4. Steady-state polarization curves of DME oxidation reaction versus DHE.

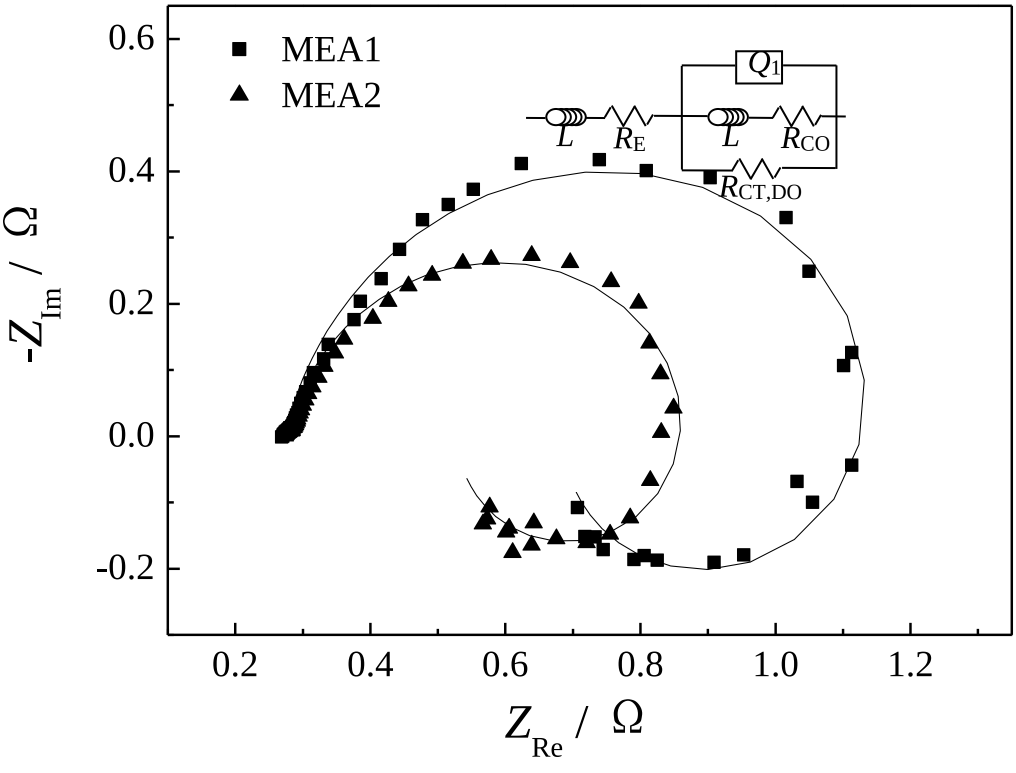

Figure 5. Electrochemical impedance spectra of DDFC anode with different catalyst (dots) and fitting diagrams using equivalent circuit (lines) at 0.45 V vs. DHE.

The EIS of anodes with different catalyst are shown in Fig.5. A possible equivalent circuit in Fig.5 is used to describe the anode process [18-20]. The fitting results analyzed by ZSimpWin software

are listed in Table 2. As seen in Fig.4, both MEA1 and MEA2 operate in low current region when the anode potential is 0.45 V vs. DHE. The mass transport polarization effect can be ignored in low current region. In Fig.5, the semicircle is due to DME oxidation reaction and the inductance in the low frequency region corresponds to the slow relaxation of CO_{ADS}. R_E is the ohmic resistance of anode. The R_E values of MEA1 and MEA2 are nearly the same. $R_{CT,DOR}$ is the charge transfer resistances of DME dehydrogenation. The $R_{CT,DOR}$ of MEA1 and MEA2 is 1.03 Ω and 0.64 Ω, respectively. R_{CO} is the charge transfer resistances of CO_{ADS} oxidation. The R_{CO} of MEA1 and MEA2 is 0.69 Ω and 0.41 Ω, respectively. The decrease of $R_{CT,DOR}$ means that DME dehydrogenation of MEA2 is easier than that of MEA1. The decrease of R_{CO} means that poisoning of the Pt in MEA2 is much more muted than that in MEA1. The total anode reaction resistance ($R_{R,A}$) of MEA1 and MEA2 is 0.41 Ω and 0.25 Ω, respectively. The increase of DDFC performance can be attributed to the decrease in the anode reaction resistance including DME dehydrogenation resistance and CO_{ADS} intermediate oxidation resistance.

Table 2. Fitting results of the resistance elements.

Resistances / Ω	MEA1	MEA2
R_E	0.27	0.28
$R_{CT, DOR}$	1.03	0.64
R_{CO}	0.69	0.41
$R_{R,,A} = (R_{CT, DOR}^{-1} + R_{CO}^{-1})^{-1}$	0.41	0.25

The amperometric *i–t* curves in Fig. 6 are used to evaluate the activity of catalyst for DME oxidation. The final current density of MEA1 and MEA2 is 26 and 42 mA cm^{-2}, respectively. The electrocatalytic activity of the mixed catalyst is higher than Pt /C. There is less drop in activity of the mixed catalyst during the whole 1000s test, which indicate that the mixed catalyst can enhance the CO-tolerance ability for the existence of Pt-Ru/C. In addition, the mixed catalyst can supply continuous Pt active sites for DME oxidation by the existence of Pt /C.

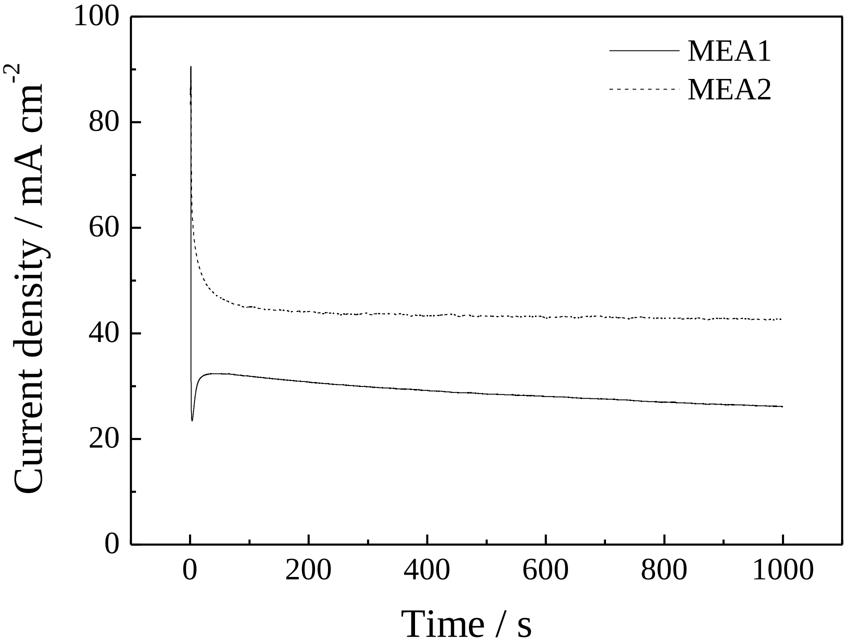

Figure 6. The amperometric *i–t* curves of DME oxidation reaction measured at 0.45 V vs. DHE.

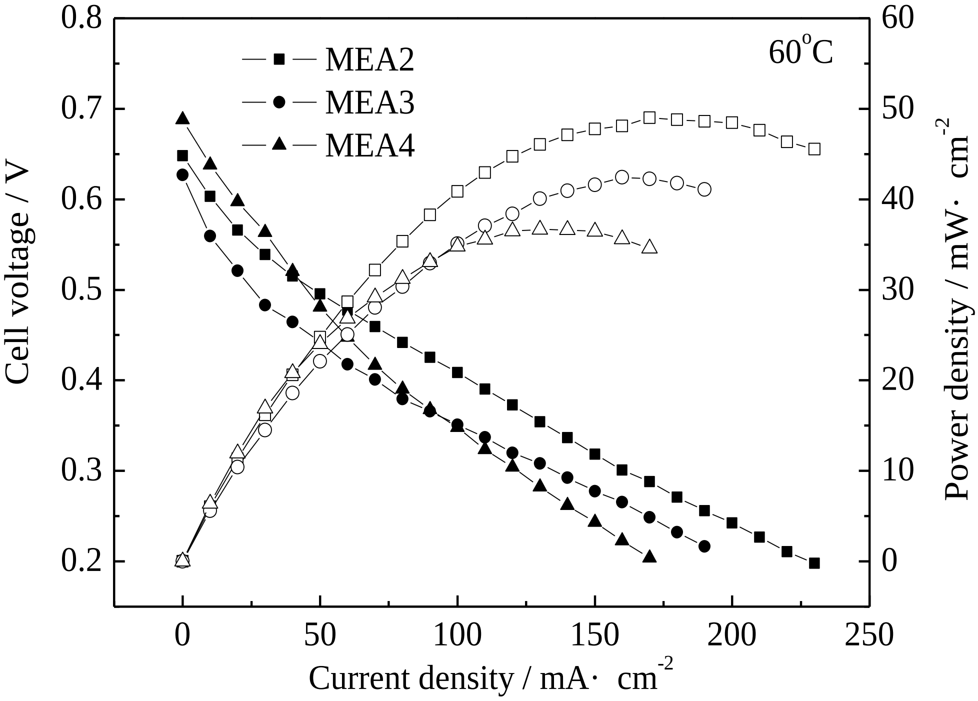

Figure 7. The polarization curves and the power density curves of MEAs with various Pt-Ru/C content in anode catalyst layer.

Fig. 7 shows the polarization curves and the power density curves of MEAs with different Pt-Ru/C content at anode. The Pt and Pt-Ru loading in anode catalyst layer of these MEAs are listed in Table 1. The MEAs perform firstly better and then worse with the increase of the Pt-Ru content in anode catalyst layer. The MEA2 with 3.5 mg cm^{-2} Pt and 0.5 mg cm^{-2} Pt-Ru in catalyst layer exists the highest output performance, and its maximum power density is 50 mW cm^2. The open circuit potentials and polarization curves (in low current density region) of different MEAs are enhanced with the increase of Ru content in anode catalyst layer. It indicates that, in low current density region, catalyst posing effect plays a major role in DME oxidation reaction. In high current density region, the oxidation of DME needs large amount of continuous Pt active sites. Too much Ru can reduce the continuous Pt active sites. The anode mixed catalyst with 3.5 mg cm^{-2} Pt and 0.5 mg cm^{-2} Pt-Ru in catalyst layer can provide continuous Pt active sites for DME dehydrogenation, and simultaneously provide oxygen-containing species to oxidize the poisoning adsorbed intermediates.

The new table has been made to compare the DME electrocatalysts described in literatures. The comparisons of these works are listed in table 3[7-10]. Comparing to these works in table 3, DDFC with Pt/C and Pt-Ru/C mixed catalyst shows higher performance under ambient pressure.

Table 3. The performances of DDFCs with different anode catalysts reported in literatures and this work

	Catalyst	The maximum power density/ mW cm^{-2}	Temperature/ ^{o}C	Pressure/bar	Reference
1	PtCu	13.5	80	1	21
2	Pt/C	60	80	3	22
3	PtRu	38	80	1	23
4	Pt/SnO$_2$/C	49.6	70	1	15
5	Mixed catalyst	60	60	1	this work

4. CONCLUSIONS

The mixed catalyst with Pt/C and Pt-Ru/C are prepared for DME oxidation in DDFC. TEM tests show that the average sizes of Pt and Pt-Ru alloy nanoparticles are nearly the same (about 3 nm). the EIS results show that the addition of Ru can reduce $R_{\mathrm{CT,DOR}}$ and R_{CO} of DME oxidation reaction. The mixed catalyst is helpful for reducing the catalyst poisoning effect, and simultaneously can provide continuous Pt active sites for DME dehydrogenation. Too much content Pt-Ru in mixed catalyst can reduce the catalytic activity. DDFC with 3.5 mg cm^{-2} Pt and 0.5 mg cm^{-2} Pt-Ru in anode catalyst layer shows the highest performance (50 mW cm^{-2}).

ACKNOWLEDGEMENT
This work was supported by University Nursing Program for Young Scholars with the Young Scholars Programs of Mu Danjiang Normal University (GG2018001), Creative Talents in Heilongjiang Province (UNPYSCT-2016108), the Teaching reform Projects of Mu Danjiang Normal University (19-XJ21008, KCSZ2020021), Innovation Project of University Students (202010233015).

References

1. Z. Yuan, W.Q. Wang, H.Y. Wang, and N. Razmjooy, *Energy Rep.,* 6 (2020) 662.
2. W. Sun, W.Q. Zhang, H.N. Su, P. Leung, L. Xing, L. Xu, C.Z. Yang, and Q. Xu, *Int. J. Hydrog. Energy,* 44 (2019) 32231.
3. N. Mahamai, T. Prom-anan, and T. Sarakonsri, *Mater. Today,* 17 (2019) 1561.
4. Z.B. Wang, P.J. Zuo, G.P. Yin, *Fuel Cells,* 9 (2009) 106.
5. L.H. Xing, Z.B. Wang, C.Y. Du, and G.P. Yin, *Int. J. Energy Research,* 36 (2012) 886.
6. L.H. Xing, Y.Z. Gao, Z.B. Wang, C.Y. Du, and G.P. Yin, *Int. J. Hydrog. Energy,* 36 (2011) 11102.
7. K.D. Cai, C. Wang, W.H. Pu, Y. Gao, and Z.Q. Mao, *Int. J. Hydrog. Energy,* 37 (2012) 12605.
8. C. Noack, J. Kallo, and A. K. Friedrich, *J. Appl. Electrochem.,* 42 (2012) 883.
9. L.L. Lu, G.P. Yin, Z.B. Wang, K.D. Cai, and Y.Z. Gao, *Catal. Commun.,* 10 (2009) 971.
10. K.D. Cai, G.P. Yin, J.J. Wang, and L.L. Lu, *Energy and Fuels,* 23 (2009) 903.
11. Y. Liu, S. Mitsushima, K.I. Ota, and N. Kamiya, *Electrochim. Acta,* 51 **(**2006) 6503.
12. G. Kerangueven, C. Coutanceau, E. Sibert, J. M. Leger, and C. Lamy, *J. Power Sources,* 157 (2006) 318.
13. Y. Tsutsumi , Y. Nakano , S. Kajitani , and S. Yamasita, *Electrochemistry,* 70 (2002) 984.
14. Q. Li, G. Wu, C.M. Johnston, and P. Zelenay, *Electrocatalysis,* 5 (2014) 310.
15. L.H. Xing, Y.X. Wang, C. Sui, and N. Zhang, *Int. J. Electrochem. Sci.,* 15 (2020) 2375.
16. L.H. Xing, G.P. Yin, C.Y. Du, S.X. Cui, M.H Zuo, and H.P. Wang, *Int. J. Hydrog. Energy,* 42 (2017) 16695.
17. L.H. Xing, G.P. Yin, Z.B. Wang, S. Zhang, Y.Z. Gao, and C.Y. Du, *J. Power Sources,* 198 (2012) 170.
18. J.T. Müller, P.M. Urban, and W.F. Hölderich, *J. Power Sources,* 84 (1999) 157.
19. S. Tominaka, N. Akiyama, T. Momma, and T. Osakaa, *J. Electrochem. Soc.,* 154 (2007) B902.
20. P. Liu, G.P. Yin, and K.D. Cai, *Electrochim. Acta,* 54 (2009) 6178.
21. B. Gavriel, R. Sharabi, and L. Elbaz, *ChemSusChem*, 10 (2017) 3069.
22. L. Du, S.F Lou, G.Y Chen, G.X. Zhang, F.P Kong, Z.Y. Qian, C.Y. Du, Y.Z Gao, S.H. Sun, and G.P. Yin, *J. Power Sources,* 433 (2019) 126690.
23. J.Y. Im, B.S. Kim, H.G. Choi, and S.M. Cho, *J. Power Sources,* 179 (2009) 301.